

UCSF

UC San Francisco Previously Published Works

Title

Vascular Endothelial Growth Factor C for Polycystic Kidney Diseases

Permalink

<https://escholarship.org/uc/item/2pm825x1>

Journal

Journal of the American Society of Nephrology, 27(1)

ISSN

1046-6673

Authors

Huang, Jennifer L

Woolf, Adrian S

Kolatsi-Joannou, Maria

et al.

Publication Date

2016

DOI

10.1681/asn.2014090856

Peer reviewed

Vascular Endothelial Growth Factor C for Polycystic Kidney Diseases

Jennifer L. Huang,* Adrian S. Woolf,[†] Maria Kolatsi-Joannou,* Peter Baluk,[‡] Richard N. Sandford,[§] Dorien J.M. Peters,^{||} Donald M. McDonald,[‡] Karen L. Price,* Paul J.D. Winyard,* and David A. Long*

*Developmental Biology and Cancer Programme, UCL Institute of Child Health, London, United Kingdom; [†]Institute of Human Development, Faculty of Medical and Human Sciences, University of Manchester, United Kingdom; [‡]Cardiovascular Research Institute, Comprehensive Cancer Center, and Department of Anatomy, University of California, San Francisco, California; [§]Academic Department of Medical Genetics, University of Cambridge School of Clinical Medicine, Cambridge, United Kingdom; and ^{||}Department of Human Genetics, Leiden University Medical Center, Leiden, The Netherlands

ABSTRACT

Polycystic kidney diseases (PKD) are genetic disorders characterized by progressive epithelial cyst growth leading to destruction of normally functioning renal tissue. Current therapies have focused on the cyst epithelium, and little is known about how the blood and lymphatic microvasculature modulates cystogenesis. Hypomorphic *Pkd1^{nl/nl}* mice were examined, showing that cystogenesis was associated with a disorganized pericyclic network of vessels expressing platelet/endothelial cell adhesion molecule 1 and vascular endothelial growth factor receptor 3 (VEGFR3). The major ligand for VEGFR3 is VEGFC, and there were lower levels of *Vegfc* mRNA within the kidneys during the early stages of cystogenesis in 7-day-old *Pkd1^{nl/nl}* mice. Seven-day-old mice were treated with exogenous VEGFC for 2 weeks on the premise that this would remodel both the VEGFR3⁺ pericyclic vascular network and larger renal lymphatics that may also affect the severity of PKD. Treatment with VEGFC enhanced VEGFR3 phosphorylation in the kidney, normalized the pattern of the pericyclic network of vessels, and widened the large lymphatics in *Pkd1^{nl/nl}* mice. These effects were associated with significant reductions in cystic disease, BUN and serum creatinine levels. Furthermore, VEGFC administration reduced M2 macrophage pericyclic infiltrate, which has been implicated in the progression of PKD. VEGFC administration also improved cystic disease in *Cys1^{cpk/cpk}* mice, a model of autosomal recessive PKD, leading to a modest but significant increase in lifespan. Overall, this study highlights VEGFC as a potential new treatment for some aspects of PKD, with the possibility for synergy with current epithelially targeted approaches.

J Am Soc Nephrol 27: 69–77, 2016. doi: 10.1681/ASN.2014090856

Polycystic kidney diseases (PKD) are genetic disorders, usually caused by mutations affecting proteins located in primary cilia and other regions within epithelial cells.¹ Epithelial turnover, adhesion, secretion, polarity, and ciliary functions are altered in PKD and therapies have predominantly targeted these

processes.¹ Much less is known about how the blood and lymphatic microvasculature surrounding kidney tubules might modulate cystogenesis. Previous studies using corrosion casting and angiography show that the vessels surrounding cysts in patients with autosomal dominant PKD are tortuous, abnormally

patterned, and dilated.^{2,3} Two further studies have blocked vascular endothelial growth factor A (VEGFA) signaling, a potent pro-angiogenic factor, in a non-orthologous rat PKD model but gave contradictory results and did not examine the effect of this intervention on the microvasculature.^{4,5}

We examined the blood and lymphatic microvasculature in *Pkd1^{nl/nl}* mice, which carry two hypomorphic alleles of *Pkd1*⁶ the mouse homolog of the gene most commonly mutated in human autosomal dominant PKD. Small cysts were found in the kidneys of 1-day-old *Pkd1^{nl/nl}* mice, which became more prominent 1 week postnatally; larger cysts were observed at 3 weeks, which reached a maximum at 5 weeks of age (Figure 1, A–E). In wild-type mice, there was a fine reticular network of vessels around kidney tubules as

Received September 4, 2014. Accepted March 11, 2015.

Published online ahead of print. Publication date available at www.jasn.org.

Correspondence: Dr. David A. Long, Developmental Biology and Cancer Programme, UCL Institute of Child Health, 30 Guilford Street, London, WC1N 1EH, UK. Email: d.long@ucl.ac.uk

Copyright © 2016 by the American Society of Nephrology

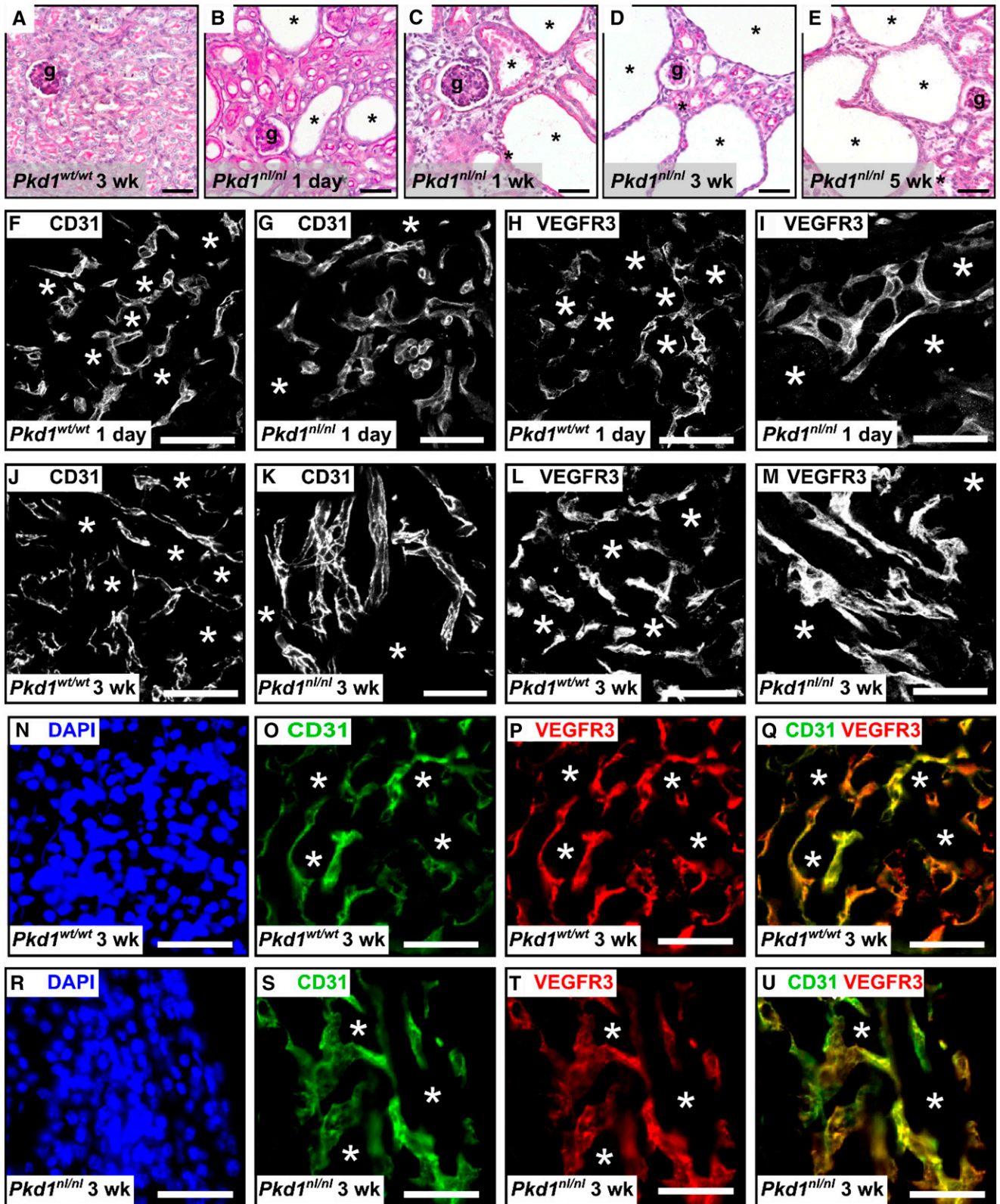


Figure 1. Disorganization of the renal microvasculature in *Pkd1*^{nl/nl} mice. (A–E) Histology of kidneys obtained from *Pkd1*^{wt/wt} and *Pkd1*^{nl/nl} mice. Representative images of immunohistochemical staining for CD31 in the kidney of a 1-day-old *Pkd1*^{wt/wt} mouse (F) and *Pkd1*^{nl/nl} mouse (G) showing the microvasculature surrounding the tubules (*). Staining for VEGFR3 in 1-day-old *Pkd1*^{wt/wt} (H) and *Pkd1*^{nl/nl} (I) mouse kidneys. Note that the CD31 and VEGFR3 frames shown for *Pkd1*^{wt/wt} and *Pkd1*^{nl/nl} mice are not of the same section. (J–M) Representative

identified by immunohistochemistry for a pan-endothelial marker, platelet/endothelial cell adhesion molecule 1 (CD31) (Figure 1, F and J). In 1-day-old littermate *Pkd1^{nl/nl}* mice there was an increase in the CD31⁺ area of noncystic renal tissue (25.7%±4.9 and 38.9%±0.7 in *Pkd1^{wt/wt}* and *Pkd1^{nl/nl}*, respectively; $P<0.05$, $n=4/\text{group}$) but no changes in the pattern of these vessels compared with *Pkd1^{wt/wt}* mice (Figure 1G). At 3 weeks of age, the pattern of CD31⁺ vessels was disrupted in *Pkd1^{nl/nl}* mice, with clusters of tortuous vessels around cysts (Figure 1K) and an increased percentage area compared with *Pkd1^{wt/wt}* animals (Supplemental Table 1). Despite the increased relative area occupied by the vessels, proliferating (CD31⁺/Ki67⁺) endothelial cells per unit area were significantly reduced in polycystic kidneys (Supplemental Table 1).

Lymphatics were identified using a panel of markers including VEGF receptor 3 (VEGFR3), podoplanin, lymphatic vessel endothelial hyaluronan receptor 1 (LYVE1) and prospero homeobox 1 (PROX1). All four proteins colocalized in large intrarenal periarterial lymphatics in both wild-type and *Pkd1^{nl/nl}* 3-week-old mice and there was no change in transverse areas with PKD (Supplemental Figure 1, Supplemental Table 1). Intriguingly, we noted a second population of VEGFR3⁺ vessels that were negative for LYVE1, podoplanin, and PROX1. These were widely distributed in peritubular areas in wild-type mice (Figure 1H, and L). In 1-day postnatal *Pkd1^{nl/nl}* kidneys, the VEGFR3⁺ area of noncystic renal tissue was increased (18.7%±1.9 and 27.4%±3.7 in *Pkd1^{wt/wt}* and *Pkd1^{nl/nl}* mice; $P<0.05$, $n=4/\text{group}$) but with no apparent changes in the pattern of the vessels compared with *Pkd1^{wt/wt}* mice (Figure 1I). At 3 weeks of age, the pattern of the peritubular VEGFR3⁺ vessels in *Pkd1^{nl/nl}* mice was disorganized

(Figure 1M) with increased percentage area (Supplemental Table 1). The VEGFR3⁺ patterns mimicked the CD31⁺ distribution pattern and using double labeling we demonstrated colocalization of CD31 and VEGFR3 in the same vessels in 3-week-old wild-type and cystic mice (Figure 1, N–U). We postulate that these CD31⁺/VEGFR3⁺ vessels may be a kidney-equivalent to specialized capillaries seen in endocrine glands,^{7,8} with molecular features shared with lymphatic endothelia and high permeability facilitating the reabsorption of glomerular filtrate into the circulation in healthy kidneys.⁹

Subsequently, we hypothesized that targeting the microvasculature may alter PKD. We decided to focus on VEGFC, which enhances growth, survival and migration of adult lymphatic endothelia through actions on VEGFR3 with lesser effects on blood vessels via VEGFR2.^{10–12} VEGFC would not only target the disorganized VEGFR3⁺ pericyclic vessels but also the larger VEGFR3⁺ lymphatics, allowing us to modulate both of these vessel types. First, we examined endogenous *Vegfc* in *Pkd1^{nl/nl}* kidneys and found a significant decrease in *Vegfc* mRNA levels at day 7 ($P<0.01$) but no difference at day 14 or 21 compared with *Pkd1^{wt/wt}* mice (Figure 2A). We then provided exogenous VEGFC to 7-day-old *Pkd1^{wt/wt}* mice by administering 100 ng/g body wt of recombinant VEGFC or vehicle intraperitoneally every day for 2 weeks (Figure 2B), a period when there is rapid growth in the size of *Pkd1^{nl/nl}* kidneys (Supplemental Figure 2). This dose has been used for VEGFA to promote renal angiogenesis¹³ and a higher dose (200 ng/g body wt) of VEGFC enhances VEGFR3 phosphorylation *in vivo*.¹⁴ We found that VEGFC administration enhanced tyrosine phosphorylation of VEGFR3 in *Pkd1^{nl/nl}* kidneys versus those given PBS (Figure 2C). VEGFC-treated *Pkd1^{nl/nl}* mice had

reduced severity of PKD as assessed by the external appearance of kidneys at autopsy (Figure 2D) and a significant approximate halving in kidney/body weight ratio (Figure 2E). *Pkd1^{nl/nl}* mice receiving VEGFC had similar body weights to those given vehicle but their absolute kidney weights were about half that of the untreated PKD littermates (1.2 g±0.3 and 0.6 g±0.2 in *Pkd1^{nl/nl}* given PBS and VEGFC, $P<0.05$). Kidneys of VEGFC-treated animals contained less prominent cysts by histology (Figure 2, F–I) with significantly smaller average cyst size (Figure 2J). VEGFC did not alter BUN and creatinine (Figure 2, K and L) concentrations in *Pkd1^{wt/wt}* animals; both of these parameters were strikingly increased in *Pkd1^{nl/nl}* mice given PBS, which was attenuated by VEGFC treatment. As a potential confounder, BUN can be lowered if there is liver damage but VEGFC did not affect plasma alanine aminotransferase levels (Figure 2M). In addition, VEGFC administration did not alter the histology of the heart, lung, liver and spleen (Figure 2, N–U).

Therapy with VEGFC had two effects on the vasculature in *Pkd1^{nl/nl}* mice. First, it increased the numbers of VEGFR3⁺/Ki67⁺ and CD31⁺/Ki67⁺ proliferating endothelial cells per unit area (Supplemental Table 1). The pattern (Figure 3, A–F) and percentage area (Supplemental Table 1) of the CD31⁺ and VEGFR3⁺ vessels in *Pkd1^{nl/nl}* mice treated with VEGFC was more like that observed in normal kidneys. Second, VEGFC significantly increased the transverse area of the larger LYVE1⁺/Prox1⁺ lymphatics in the kidney (Supplemental Table 1). However, VEGFC treatment did not significantly alter endogenous kidney mRNA levels of *Vegfa*, *Vegfc*, *Vegfr2*, or *Vegfr3* or protein levels of VEGFC (Supplemental Figure 3).

Next, we examined if these changes in the blood and lymphatic microvasculature

images of CD31 and VEGFR3 immunohistochemistry in 3-week-old *Pkd1^{wt/wt}* and *Pkd1^{nl/nl}* mouse kidneys. (N–U) Double-labeling for CD31 and VEGFR3 in the same sections of *Pkd1^{wt/wt}* and *Pkd1^{nl/nl}* mice demonstrated colocalization of both markers on vessels surrounding the kidney tubules. Bar is 50 μm in each panel, g, glomerulus.

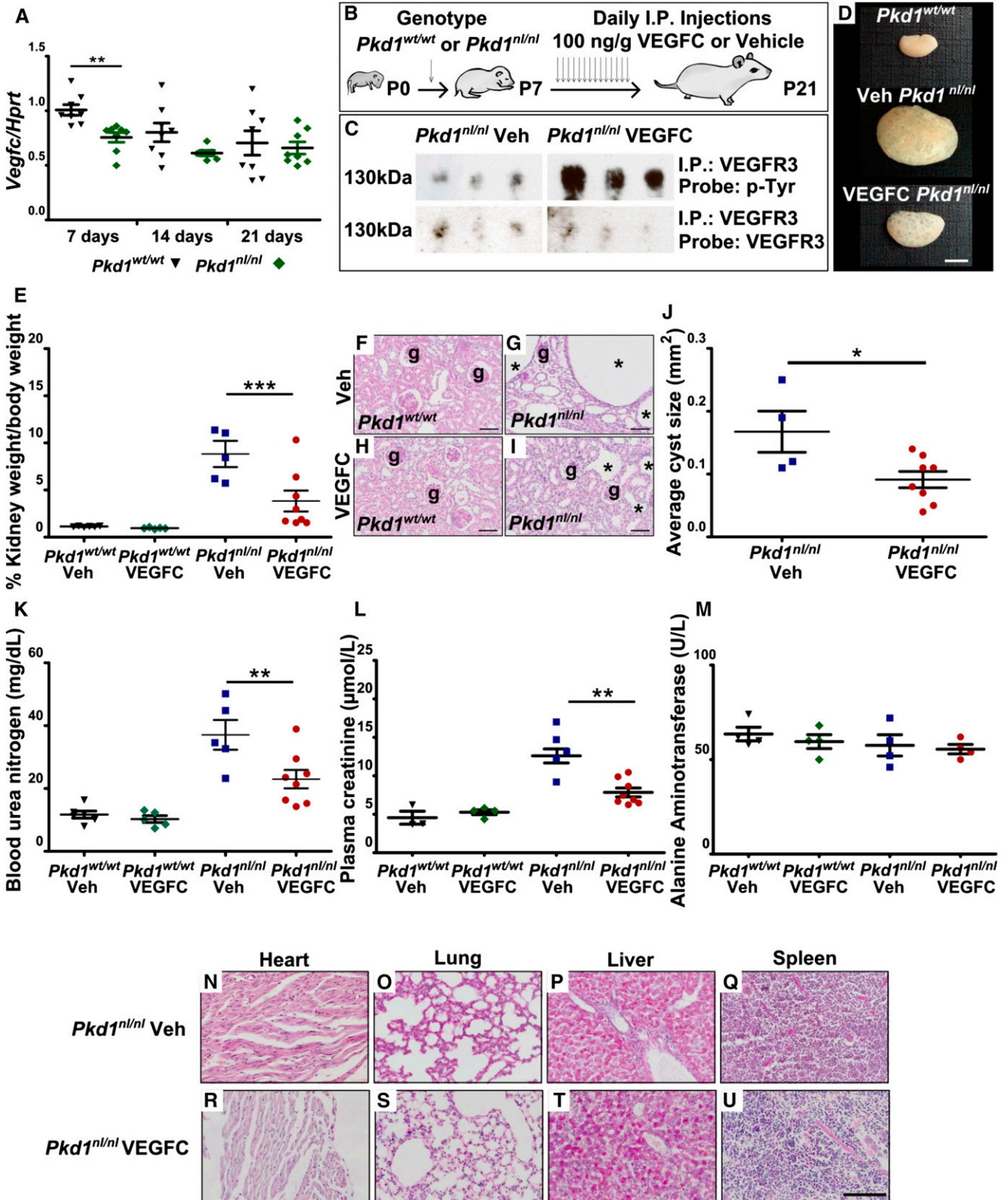


Figure 2. Administration of VEGFC to *Pkd1^{nl/nl}* mice improves kidney histology and function. (A) Quantitative RT-PCR comparing mRNA levels of *Vegfc* in *Pkd1^{wt/wt}* and *Pkd1^{nl/nl}* mouse kidneys at 7, 14, and 21 days after birth. All data are presented relative to levels in *Pkd1^{wt/wt}* kidney at day 7 where average expression was given an arbitrary value of 1. (B) Outline of experimental strategy. (C) VEGFR3 phosphorylation levels in the kidneys of *Pkd1^{nl/nl}* mice given either vehicle or VEGFC. (D) Representative images showing overall appearance of

might correlate with the inflammatory milieu in PKD by examining CD206/*Mrc1*⁺ alternatively activated macrophages (M2), which have been functionally implicated in PKD cyst growth.^{15,16} VEGFC significantly reduced these cells in *Pkd1*^{nl/nl} mice (Figure 3, G–J). Treatment also led to significantly lower renal *Mrc1* levels in *Pkd1*^{nl/nl} mice (Figure 3K) although the reduction of another M2 marker, arginase 1 (*Arg1*), did not reach significance (Figure 3L). In contrast, none of the M1 macrophage markers tested were affected by VEGFC administration (Figure 3, M and N). Similarly, the extent of fibrosis was unaffected, as assessed by mRNA for collagen type III, $\alpha 1$ (*Col3a1*) (Figure 3O).

The normalization of the pericycystic network of vessels alongside reduced inflammatory macrophages suggest that the microvasculature is the prime target of VEGFC therapy, but the same results might be generated as secondary effects if the growth factor acted directly on cystic epithelia. However, VEGFC did not alter proliferation in small cysts (<0.01 mm²; 29 ± 6 versus 33 ± 3 proliferating nuclei/500 cells in *Pkd1*^{nl/nl} mice treated with PBS and VEGFC) with few Ki67⁺ cells detected in cysts larger than this in all experimental groups. In contrast to previous reports,^{3,4,17} we could not detect the VEGFC receptors VEGFR2 or VEGFR3 on the cyst epithelia by immunohistochemistry in multiple animals; contrasting markedly with clear expression in vessels on the same section (Figure 3, P and Q). Hence, we conclude that the prime effects of VEGFC are likely to be vascularly targeted, although we cannot fully rule out epithelial effects that could be evaluated using isolated cyst models. It will be worth re-examining the VEGFA pathway in future experiments. Previous

studies were performed in Han:SPRD rats, a model which does not harbor a human PKD-relevant mutation,¹⁸ with anti-VEGFA antibody causing worse renal function and enhanced kidney injury in one laboratory⁵ whereas ribozymes to block VEGFR1 and VEGFR2 reduced cyst volume density and improved renal function in another.⁴ An explanation for these findings is that simply blocking VEGFA is known to cause profound glomerular changes¹⁹ and the effects on cystic tubules could be secondary to these. The blockade of VEGFR2 by ribozymes may favor endogenous VEGFC binding to VEGFR3⁺ vessels, which our study has shown to be beneficial.

We questioned whether the positive effects of VEGFC are specific for *Pkd1* mutants or have more widespread effects on cystogenesis by using mice with congenital polycystic kidneys (*Cys1*^{cpk/cpk} mice). This model is nonorthologous, but provides a rapid phenocopy of the pathology of human autosomal recessive PKD with massive collecting duct cystogenesis leading to uremic death by 3 weeks of age.²⁰ First, we examined 2-week-old *Cys1*^{cpk/cpk} mice and found that the CD31⁺ and VEGFR3⁺ pericycystic network of vessels were also disorganized compared with *Cys1*^{+/+} mice and that both markers colocalized (Supplemental Figure 4). The relative area occupied by the VEGFR3⁺ vessels was significantly increased in *Cys1*^{cpk/cpk} mice compared with wild-type littermates with a tendency for this to be the case for CD31⁺ vessels (Supplemental Table 2). VEGFC was again provided daily from postnatal day 7 to day 14 (Figure 4A); a phase where there is rapid growth in the size of *Cys1*^{cpk/cpk} kidneys (Supplemental Figure 3). VEGFC administration to *Cys1*^{cpk/cpk} mice led to an improvement in gross morphology (Figure 4B) and a

significant reduction in kidney/body weight ratio compared with those treated with PBS (Figure 4C). *Cys1*^{cpk/cpk} receiving VEGFC had similar body weights to those given PBS but had a significantly lower kidney weight ($0.6 \text{ g} \pm 0.1$ and $0.5 \text{ g} \pm 0.1$ in *Cys1*^{cpk/cpk} mice treated with PBS and VEGFC, $P < 0.05$). VEGFC treatment, did not, however, affect BUN concentration (Figure 4D). Kidneys of VEGFC-treated *Cys1*^{cpk/cpk} mice had less prominent cysts (Figure 4, E–H) with a significantly smaller average cyst size (Figure 4I). VEGFC increased the number of proliferating CD31⁺ and VEGFR3⁺ vessels in *Cys1*^{cpk/cpk} mice (Supplemental Table 2), which was associated with a reduction in the VEGFR3⁺ percentage area (Supplemental Table 2). VEGFC administration did not alter the average cross-sectional area of the larger LYVE1⁺/Prox1⁺ lymphatics in *Cys1*^{cpk/cpk} mice. Finally, VEGFC treatment led to a modest but significantly extended survival of 1 week in *Cys1*^{cpk/cpk} mice (Figure 4J).

In conclusion, this study shows that an abnormal pericycystic network of vessels is present from the early stages of PKD and becomes more disorganized as cystogenesis progresses. We demonstrated that intervening with VEGFC enhances the phosphorylation of VEGFR3, which has been shown to lead to the proliferation, migration and rearrangement of vessels.²¹ VEGFC treatment also reduces the severity of PKD, which is associated with improving the pattern of the pericycystic vascular network, widening the large lymphatics and clearing inflammatory cells. The combination of these effects may have the potential to reduce edema, which is a regular feature of PKD.²² We do not yet understand why the kidney microvasculature is abnormal in PKD. One reason is that the vessels are

kidneys from *Pkd1*^{wt/wt} and *Pkd1*^{nl/nl} mice given either vehicle or VEGFC. Bar is 0.5 cm for each panel. (E) Assessment of kidney/body weight ratio. (F–I) Representative images of periodic acid–Schiff-stained kidney sections obtained from *Pkd1*^{wt/wt} and *Pkd1*^{nl/nl} mice given either vehicle or VEGFC; g, glomerulus; * tubule. (J) Analysis of average area of individual cysts. (K) Assessment of BUN, creatinine concentration (L) and serum alanine aminotransferase (M). (N–U) Histology of the heart, lung, liver, and spleen from *Pkd1*^{nl/nl} mice given either vehicle or VEGFC. In each group and analysis, $n = 4$ to $n = 8$; data are presented as mean \pm SEM. * $P < 0.05$; ** $P < 0.01$; and *** $P < 0.001$ between groups. Bar represents 50 μm in each panel.

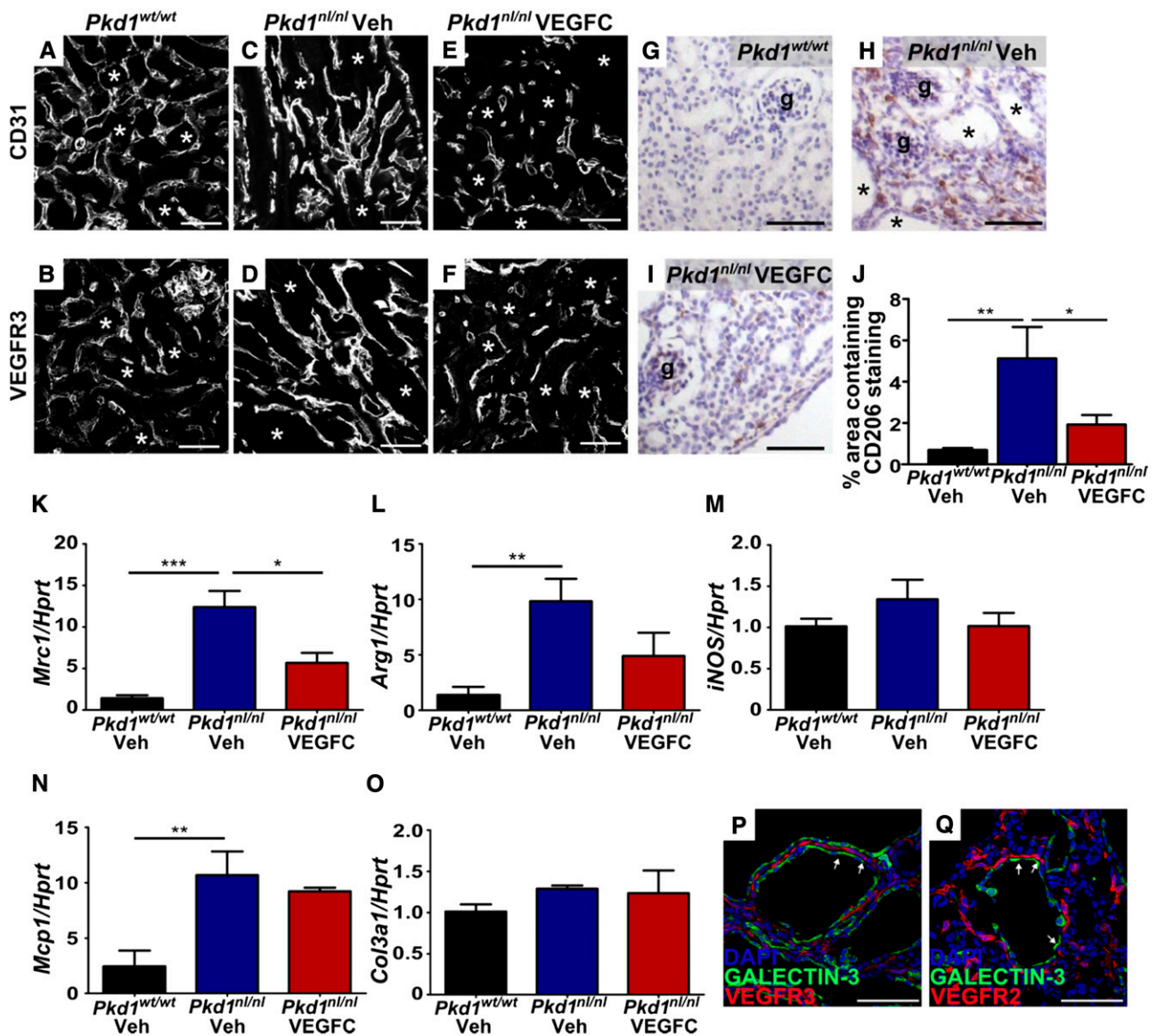


Figure 3. VEGFC administration modulates the renal vasculature and reduces inflammation in *Pkd1*^{nl/nl} mice. *Pkd1*^{wt/wt} mice contained CD31⁺ and VEGFR3⁺ vessels arranged in a delicate linear network surrounding the kidney tubules (indicated by * in [A] and [B]); these vessels were disrupted in untreated *Pkd1*^{nl/nl} mice (C,D) whereas administration of VEGFC to *Pkd1*^{nl/nl} mice normalized these aberrant patterns (E,F). (G–I) Immunostaining for CD206-positive cells revealed prominent expression in the interstitial tissue surrounding cysts (*), but not in glomeruli (g) in *Pkd1*^{nl/nl} mice, which was diminished after VEGFC therapy. Quantification of CD206-positive cells (J), *n*=5 to *n*=8 in each group. mRNA levels of *Mrc1* (K), *Arg1* (L), *iNOS* (M), *Mcp1* (N), and *Col3a1* (O) assessed by quantitative real-time PCR and presented relative to levels in *Pkd1*^{wt/wt} kidneys, *n*=4 in each group (P, Q). Double-labeling in 3-week-old *Pkd1*^{nl/nl} mice given vehicle with antibodies to detect either VEGFR2 or VEGFR3 and galectin-3, a marker for cyst epithelial cells derived from the collecting duct (arrows). All data are presented as mean ± SEM. **P*<0.05; ***P*<0.01; and ****P*<0.001 between groups. Bar represents 50 μm in each panel.

simply distorted as cysts grow. Alternatively, there may be intrinsic defects in the vasculature, as has been reported in the skin lymphatics in *Pkd1*-null and *Pkd2*-null mice,²² which may explain why the effects of VEGFC are more prominent in *Pkd1*^{nl/nl} mice than *Cys1*^{cpk/cpk}. Other studies have also demonstrated a

role for *Pkd1* in zebrafish lymphatic vessel morphogenesis²³

Future experiments should investigate VEGFC and other vascular growth factors perhaps in combination with epithelially targeted treatments. Ideally, these studies should include a slow-onset orthologous PKD1 model such as the *Pkd1*^{RC/RC}

mouse,²⁴ since both of the models examined here progress very quickly, which did not allow the examination of multiple stages of cyst initiation, progression and end-stage PKD. In addition, detailed studies need to be performed to determine optimal doses and timing periods for VEGFC treatment. Combining epithelial and

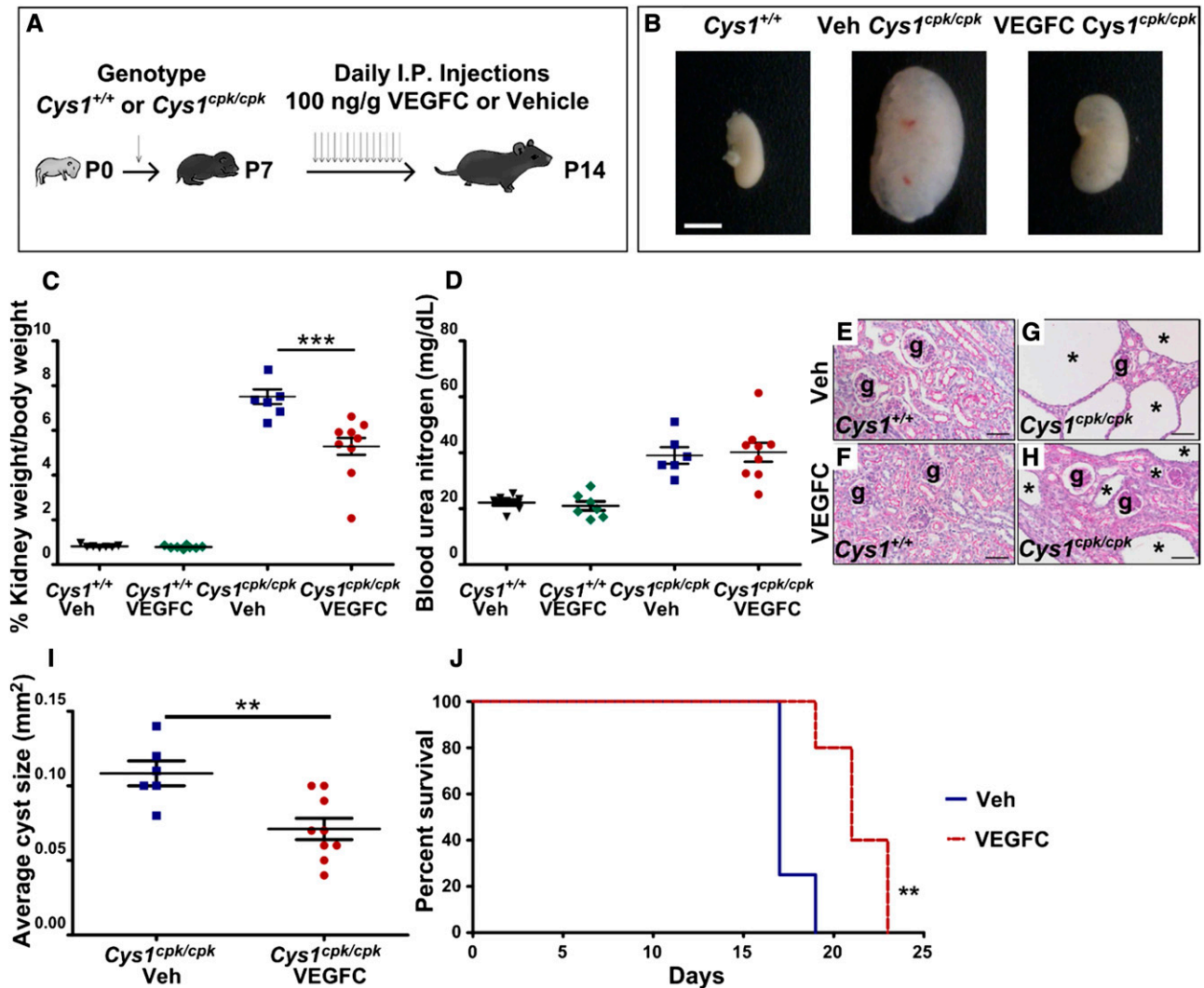


Figure 4. VEGFC treatment improves kidney histology and survival in $Cys1^{cpk/cpk}$ mice. (A) Outline of experimental strategy. (B) Representative images showing overall appearance of kidneys from $Cys1^{+/+}$ and $Cys1^{cpk/cpk}$ mice given either vehicle or VEGFC. Bar is 0.5 cm for each panel. (C) Assessment of kidney/body wt ratio and (D) BUN concentration. (E–H) Representative images of periodic acid–Schiff-stained kidney sections obtained from $Cys1^{+/+}$ and $Cys1^{cpk/cpk}$ mice given either vehicle or VEGFC. Bar represents 50 μ m in each panel, g, glomerulus; * shows dilated tubule. (I) Image J particle analysis of images of whole kidneys under a dissection microscope to determine the average area of individual cysts. (J) Survival analysis of $Cys1^{cpk/cpk}$ mice administered either vehicle or VEGFC. $n=7$ to $n=11$ in each group for A–I, $n=6$ for J, data are presented as mean \pm SEM. * $P<0.05$; ** $P<0.01$; and *** $P<0.001$ between groups.

endothelial therapies may generate the effective treatments urgently needed for these important human diseases.

CONCISE METHODS

Animal Models

$Cys1^{cpk/+}$ (The Jackson Laboratory, Bar Harbor, ME)²⁰ and $Pkd1^{nl/wt}$ heterozygous mice⁶ were bred to generate wild-type and homozygous littermates for analysis. $Cys1^{cpk/+}$ mice

were maintained on the C57BL/6J background for at least 25 generations and $Pkd1^{nl/wt}$ mice were maintained on CD1 background for more than ten generations. In some experiments, wild-type and homozygous $Cys1$ and $Pkd1$ mice were injected with either 100 ng/g body wt of recombinant VEGFC (R&D Systems Europe, Abingdon, UK) or vehicle (PBS) intraperitoneally daily. The daily volume administered was 20 μ l, equivalent to providing 200 ml PBS to an adult human per day, or 20 ml/day to an infant. All animal

procedures were approved by the UK Home Office.

Assessment of Renal Function

Blood was collected and BUN was assessed using a commercially available assay kit, validated in mice.²⁵ Creatinine concentration was measured using isotope dilution electrospray mass spectrometry. Alanine aminotransferase was assessed using the Vitros 5600 clinical chemistry analyzer (Ortho Clinical Diagnostics, High Wycombe, UK).

Histologic Analysis and Immunohistochemistry

After anesthesia, the vasculature was perfused to ensure optimal tissue preservation and maintain vessel patency with 1% paraformaldehyde in PBS from a cannula inserted through the left ventricle into the aorta. Tissues were removed, fixed further by immersion in 1% paraformaldehyde for another 1 hour, washed in PBS, dehydrated and embedded in wax; then 5- μ m sections were cut. Some sections were stained with periodic acid–Schiff reagent and hematoxylin to assess the overall histology. Pictures of whole stained kidneys were taken at low magnification under a dissecting microscope and the average area of individual cysts (defined as dilated tubules >0.01 mm² in cross-sectional area) was determined using ImageJ particle analysis (<http://rsbweb.nih.gov/ij/>).²⁶ Immunohistochemistry was performed for CD206 (MCA2235T, AdB Serotec, Oxford, UK) with appropriate secondary antibodies conjugated to horseradish peroxidase and detected by 3,3'-diaminobenzidine with the color development performed for the same duration of time for each sample. Negative controls consisted of omission of primary antibodies or substitution with preimmune serum. Photomicrographs of 20 sequential fields using a $\times 20$ objective were taken and the area of the kidney cortex containing positive immunoreactivity was analyzed as a percentage of the whole image using ImmunoRatio and ImageJ software.²⁷ To circumvent any effects of cyst area on the analyses, the area occupied by dilated tubules >0.01 mm² was subtracted from each analyzed image.

In some cases after perfusion, kidneys were prepared for cryosectioning by fixing in 1% paraformaldehyde, placing samples in 30% sucrose in PBS and embedding in Tissue-Tek optimal cutting temperature compound (Sakura Finetek, Torrance, CA). Ten-micrometer sections were permeabilized in PBS containing 0.03% Triton and then incubated in PBS-Triton containing 10% normal donkey serum (Jackson ImmunoResearch Laboratories, West Grove, PA), 0.2% BSA, and 0.1% sodium azide for 1 hour at room temperature to block nonspecific antibody binding. Sections were incubated with one or more of the following primary antibodies overnight at room temperature: CD31 (MA3105; Thermo Fisher Scientific, Waltham, MA),^{28,29} galectin-3 (sc-20517; Santa Cruz

Biotechnology, Dallas, TX),³⁰ Ki67 (ab6155; Abcam, Inc., Cambridge, UK),²⁹ LYVE1 (AF2125; R&D Systems, Abingdon, Europe),³¹ podoplanin (ab11936; Abcam, Inc.),³² PROX1 (11–022; AngioBio, Del Mar, CA),²⁸ VEGFR2 (AF644; R&D Systems),³³ VEGFR3 (AF743; R&D Systems).²⁸ Serial sections were used to determine colocalization of vascular and lymphatic markers. After washing in PBS-Triton, sections were incubated with appropriate Cy3, AlexaFluor594 and AlexaFluor488 secondary antibodies and visualized by confocal microscopy. Images of whole kidney sections from fluorescently labeled slides were obtained using an Axio Scan.Z1 (Carl Zeiss, Munich, Germany) and were then quantified in ImageJ. The area of the kidney sections positive for vascular markers was calculated as a percentage of the total 4',6-diamidino-2-phenylindole⁺ area to circumvent any effects of cysts on the analyses. The numbers of proliferating CD31⁺ and VEGFR3⁺ vessels were counted and expressed as positive cell numbers/cm² of 4',6-diamidino-2-phenylindole area. To measure epithelial proliferation the number of Ki67⁺ cells was determined per 500 in at least 50 small cysts <0.01 mm²; larger cysts >0.01 mm² were also assessed. The average area occupied by LYVE1⁺/Prox1⁺ vessels was measured by analyzing at least 20 vessels in each sample.

Immunoprecipitation and Western Blotting

Five hundred micrograms of protein from kidneys of *Pkd1*^{nl/nl} mice that were given vehicle or VEGFC was isolated using RIPA buffer and incubated with Dynabead Protein G (Life Technologies, Paisley, UK) and 5 μ g of VEGFR3 (R&D Systems) antibody. Bound protein was eluted, denatured and separated on SDS–8% polyacrylamide gels. After electroblotting, proteins were detected using antibodies for phosphotyrosine (05–321, EMD Millipore, Billerica, MA) or VEGFR3 (R&D Systems). For the detection of endogenous VEGFC, 50 μ g of kidney protein was separated, electroblotted and probed using a VEGFC antibody (sc-1881; Santa Cruz Biotechnology); α -tubulin was used as a house-keeping protein and densitometry analysis was performed.

Real-Time PCR

RNA was extracted using the RNeasy kit (Qiagen, Crawley, UK) from whole kidneys; 500 ng of RNA

was used to prepare cDNA and quantitative real-time PCR was performed for *Arg1*, *Cd206*, *Col3a1*, *iNOS*, *Mcp1*, *Vegfa*, *Vegfc*, *Vegfr2*, and *Vegfr3* on a CFX96 Touch Real-Time PCR Detection System (Bio-Rad Laboratories, Ltd., Hemel Hempstead, UK) using SsoAdvanced Supermix (Bio-Rad Laboratories, Ltd.) with hypoxanthine-guanine phosphoribosyltransferase (*Hprt*) as a house-keeping gene. Fold-changes in gene expression were determined by the $2^{-\Delta\Delta CT}$ method. Primer details are available on request.

Statistical analyses

All samples were assessed blinded to treatment. Data were presented as means \pm SEM. In experiments when differences between two groups were evaluated, data were analyzed by Mann–Whitney *U* test (IBM SPSS, Chicago, IL). When three or more groups were assessed one-way ANOVA with least square difference *post hoc* test (IBM SPSS) was used. Survival analysis was presented using the Kaplan–Meier estimate and assessed by the log-rank test. Statistical significance was accepted at $P < 0.05$.

ACKNOWLEDGMENTS

We thank UCL Biological Services, GOSH Chemical Pathology and Professor Neil Dalton (King's College London) for their assistance with animal experiments, and alanine aminotransferase and creatinine measurements, respectively. We thank Professor Paul Riley (University of Oxford) and Professor Paul Gissen (UCL institute of Child Health) for helpful discussions regarding this work.

This work was supported by a studentship from Kids Kidney Research (to D.A.L., A.S.W., and P.J.D.W.), a project grant from Kidney Research UK (RP38/2013 to D.A.L. and P.J.D.W.) and a Bogue Research Fellowship to J.L.H. D.A.L. is supported by a Kidney Research UK Senior Non-Clinical Fellowship (SF1/2008) and a Medical Research Council New Investigator Award (MR/J003638/1). The contributions by Peter Baluk and Donald M. McDonald were supported in part by grants from the National Heart, Lung, and Blood Institute (P01-HL024136 and R01-HL059157) of the US National Institutes of Health. Karen L. Price is supported by the ICH/GOSH Biomedical Research Centre. Adrian S. Woolf

acknowledges grant support from the Manchester Biomedical Research Centre and the Medical Research Council (MR/K026739/1 and MR/L012707/1).

DISCLOSURES

J.L.H., P.J.D.W., and D.A.L. hold a patent related to therapies targeting the lymphatics in polycystic kidney disease.

REFERENCES

- Harris PC, Torres VE: Polycystic kidney disease. *Annu Rev Med* 60: 321–337, 2009
- Wei W, Popov V, Walocha JA, Wen J, Bello-Reuss E: Evidence of angiogenesis and microvascular regression in autosomal-dominant polycystic kidney disease kidneys: a corrosion cast study. *Kidney Int* 70: 1261–1268, 2006
- Bello-Reuss E, Holubec K, Rajaraman S: Angiogenesis in autosomal-dominant polycystic kidney disease. *Kidney Int* 60: 37–45, 2001
- Tao Y, Kim J, Yin Y, Zafar I, Falk S, He Z, Faubel S, Schrier RW, Edelstein CL: VEGF receptor inhibition slows the progression of polycystic kidney disease. *Kidney Int* 72: 1358–1366, 2007
- Raina S, Honer M, Krämer SD, Liu Y, Wang X, Segerer S, Wüthrich RP, Serra AL: Anti-VEGF antibody treatment accelerates polycystic kidney disease. *Am J Physiol Renal Physiol* 301: F773–F783, 2011
- Lantinga-van Leeuwen IS, Dauwse JG, Baelde HJ, Leonhard WN, van de Wal A, Ward CJ, Verbeek S, Deruiter MC, Breuning MH, de Heer E, Peters DJ: Lowering of Pkd1 expression is sufficient to cause polycystic kidney disease. *Hum Mol Genet* 13: 3069–3077, 2004
- Tammela T, Alitalo K: Lymphangiogenesis: Molecular mechanisms and future promise. *Cell* 140: 460–476, 2010
- Stan RV, Kubitzka M, Palade GE: PV-1 is a component of the fenestral and stomatal diaphragms in fenestrated endothelium. *Proc Natl Acad Sci U S A* 96: 13203–13207, 1999
- Fine LG: Ernest Henry Starling (1866–1927) on the formation and reabsorption of lymph. *Nephron, Physiol* 126: 9–17, 2014
- Huggenberger R, Ullmann S, Proulx ST, Pytowski B, Alitalo K, Detmar M: Stimulation of lymphangiogenesis via VEGFR-3 inhibits chronic skin inflammation. *J Exp Med* 207: 2255–2269, 2010
- Mäkinen T, Veikkola T, Mustjoki S, Karpanen T, Catimel B, Nice EC, Wise L, Mercer A, Kowalski H, Kerjaschki D, Stacker SA, Achen MG, Alitalo K: Isolated lymphatic endothelial cells transduce growth, survival and migratory signals via the VEGF-C/D receptor VEGFR-3. *EMBO J* 20: 4762–4773, 2001
- Hamada K, Oike Y, Takakura N, Ito Y, Jussila L, Dumont DJ, Alitalo K, Suda T: VEGF-C signaling pathways through VEGFR-2 and VEGFR-3 in vasculoangiogenesis and hematopoiesis. *Blood* 96: 3793–3800, 2000
- Kang DH, Hughes J, Mazzali M, Schreiner GF, Johnson RJ: Impaired angiogenesis in the remnant kidney model: II. Vascular endothelial growth factor administration reduces renal fibrosis and stabilizes renal function. *J Am Soc Nephrol* 12: 1448–1457, 2001
- Benedito R, Rocha SF, Woeste M, Zamykal M, Radtke F, Casanovas O, Duarte A, Pytowski B, Adams RH: Notch-dependent VEGFR3 upregulation allows angiogenesis without VEGF-VEGFR2 signalling. *Nature* 484: 110–114, 2012
- Karihaloo A, Koraihy F, Huen SC, Lee Y, Merrick D, Caplan MJ, Somlo S, Cantley LG: Macrophages promote cyst growth in polycystic kidney disease. *J Am Soc Nephrol* 22: 1809–1814, 2011
- Swenson-Fields KI, Vivian CJ, Salah SM, Peda JD, Davis BM, van Rooijen N, Wallace DP, Fields TA: Macrophages promote polycystic kidney disease progression. *Kidney Int* 83: 855–864, 2013
- Kanellis J, Fraser S, Katerelos M, Power DA: Vascular endothelial growth factor is a survival factor for renal tubular epithelial cells. *Am J Physiol Renal Physiol* 278: F905–F915, 2000
- Kaisaki PJ, Bergmann C, Brown JH, Outeda P, Lens XM, Peters DJ, Gretz N, Gauguier D, Bihoreau MT: Genomic organization and mutation screening of the human ortholog of Pkcd1 associated with polycystic kidney disease in the rat. *Eur J Med Genet* 51: 325–331, 2008
- Veron D, Reidy KJ, Bertuccio C, Teichman J, Villegas G, Jimenez J, Shen W, Kopp JB, Thomas DB, Tufro A: Overexpression of VEGF-A in podocytes of adult mice causes glomerular disease. *Kidney Int* 77: 989–999, 2010
- Hou X, Mrug M, Yoder BK, Lefkowitz EJ, Kremmidiotis G, D'Eustachio P, Beier DR, Guay-Woodford LM: Cystin, a novel cilia-associated protein, is disrupted in the CPK mouse model of polycystic kidney disease. *J Clin Invest* 109: 533–540, 2002
- Koch S, Claesson-Welsh L: Signal transduction by vascular endothelial growth factor receptors. *Cold Spring Harb Perspect Med* 2: a006502, 2012
- Outeda P, Huso DL, Fisher SA, Halushka MK, Kim H, Qian F, Gemino GG, Watnick T: Polycystin signaling is required for directed endothelial cell migration and lymphatic development. *Cell Reports* 7: 634–644, 2014
- Coxam B, Sabine A, Bower NI, Smith KA, Pichol-Thieuvend C, Skoczylas R, Astin JW, Frampton E, Jaquet M, Crosier PS, Parton RG, Harvey NL, Petrova TV, Schulte-Merker S, Francois M, Hogan BM: Pkd1 regulates lymphatic vascular morphogenesis during development. *Cell Reports* 7: 623–633, 2014
- Hopp K, Ward CJ, Hommerding CJ, Nasr SH, Tuan HF, Gainullin VG, Rossetti S, Torres VE, Harris PC: Functional polycystin-1 dosage governs autosomal dominant polycystic kidney disease severity. *J Clin Invest* 122: 4257–4273, 2012
- Kolatsi-Joannou M, Price KL, Winyard PJ, Long DA: Modified citrus pectin reduces galectin-3 expression and disease severity in experimental acute kidney injury. *PLoS ONE* 6: e18683, 2011
- Chan SK, Riley PR, Price KL, McElduff F, Winyard PJ, Welham SJ, Woolf AS, Long DA: Corticosteroid-induced kidney dysmorphogenesis is associated with deregulated expression of known cystogenic molecules, as well as Indian hedgehog. *Am J Physiol Renal Physiol* 298: F346–F356, 2010
- Tuominen VJ, Ruotoistenmäki S, Viitanen A, Jumppanen M, Isola J: ImmunoRatio: a publicly available web application for quantitative image analysis of estrogen receptor (ER), progesterone receptor (PR), and Ki-67. *Breast Cancer Res* 12: R56, 2010
- Yao LC, Testini C, Tvorogov D, Anisimov A, Vargas SO, Baluk P, Pytowski B, Claesson-Welsh L, Alitalo K, McDonald DM: Pulmonary lymphangiectasia resulting from vascular endothelial growth factor-C overexpression during a critical period. *Circ Res* 114: 806–822, 2014
- Dessapt-Baradez C, Woolf AS, White KE, Pan J, Huang JL, Hayward AA, Price KL, Kolatsi-Joannou M, Locatelli M, Diennet M, Webster Z, Smillie SJ, Nair V, Kretzler M, Cohen CD, Long DA, Gnudi L: Targeted glomerular angiotensin-1 therapy for early diabetic kidney disease. *J Am Soc Nephrol* 25: 33–42, 2014
- Chiu MG, Johnson TM, Woolf AS, Dahm-Vicker EM, Long DA, Guay-Woodford L, Hillman KA, Bawumia S, Venner K, Hughes RC, Poirier F, Winyard PJ: Galectin-3 associates with the primary cilium and modulates cyst growth in congenital polycystic kidney disease. *Am J Pathol* 169: 1925–1938, 2006
- Jeansson M, Gawlik A, Anderson G, Li C, Kerjaschki D, Henkelman M, Quaggin SE: Angiopoietin-1 is essential in mouse vasculature during development and in response to injury. *J Clin Invest* 121: 2278–2289, 2011
- Danussi C, Spessotto P, Petrucco A, Wassermann B, Sabatelli P, Montesi M, Doliana R, Bressan GM, Colombatti A: Emilin1 deficiency causes structural and functional defects of lymphatic vasculature. *Mol Cell Biol* 28: 4026–4039, 2008
- Lohela M, Heloterä H, Haiko P, Dumont DJ, Alitalo K: Transgenic induction of vascular endothelial growth factor-C is strongly angiogenic in mouse embryos but leads to persistent lymphatic hyperplasia in adult tissues. *Am J Pathol* 173: 1891–1901, 2008

See related editorial, "Vascular Endothelial Growth Factor Therapy for the Kidney: Are We There Yet?," on pages 1–3.

This article contains supplemental material online at <http://jasn.asnjournals.org/lookup/suppl/doi:10.1681/ASN.2014090856/-DCSupplemental>